

1 Title:

2 WEVar: a novel statistical learning framework 3 for predicting noncoding regulatory variants

4 Ye Wang^{1,2,3}, Yuchao Jiang^{4,5}, Bing Yao⁶, Kun Huang^{1,2}, Yunlong Liu^{2,7}, Yue Wang⁷, Xiao Qin³, Andrew
5 J. Saykin⁸ & Li Chen^{1,2,#}

6 ¹Department of Medicine, Indiana University School of Medicine, Indianapolis, IN, 46202

7 ²Center for Computational Biology and Bioinformatics, Indiana University School of Medicine, Indianapolis, IN, 46202

8 ³Department of Computer Science and Software Engineering, Auburn University, Auburn, AL, 36849

9 ⁴Department of Biostatistics, Gillings School of Global Public Health, University of North Carolina, Chapel Hill, NC 27599

10 ⁵Department of Genetics, School of Medicine, University of North Carolina at Chapel Hill, Chapel Hill, NC 27599

11 ⁶Department of Human Genetics, Emory University, Atlanta, GA 30322

12 ⁷Department of Medical and Molecular Genetics, Indiana University School of Medicine, Indianapolis, IN, 46202

13 ⁸Department of Radiology and Imaging Sciences, Indiana University School of Medicine, Indianapolis, IN, 46202

14 November 16, 2020

15 **Abstract**

16 Understanding the functional consequence of noncoding variants is of great interest. Though genome-wide
17 association studies (GWAS) or quantitative trait locus (QTL) analyses have identified variants associated with
18 traits or molecular phenotypes, most of them are located in the noncoding regions, making the identification
19 of causal variants a particular challenge. Existing computational approaches developed for prioritizing non-
20 coding variants produce inconsistent and even conflicting results. To address these challenges, we propose a
21 novel statistical learning framework, which directly integrates the precomputed functional scores from represen-
22 tative scoring methods. It will maximize the usage of integrated methods by automatically learning the relative
23 contribution of each method and produce an ensemble score as the final prediction. The framework consists
24 of two modes. The first “context-free” mode is trained using curated causal regulatory variants from a wide
25 range of context and is applicable to predict noncoding variants of unknown and diverse context. The second
26 “context-dependent” mode further improves the prediction when the training and testing variants are from the
27 same context. By evaluating the framework via both simulation and empirical studies, we demonstrate that it
28 outperforms integrated scoring methods and the ensemble score successfully prioritizes experimentally validated
29 regulatory variants in multiple risk loci.

30 **Keywords**— noncoding variants, prioritization, functional score

#Contact: chen61@iu.edu

31 Introduction

32 In the past decade, genome-wide association studies (GWAS) have been widely used to identify tens of
33 thousands of genome-wide significant tag SNPs associated with complex traits. However, tag SNPs may
34 not be causal as the association is possibly mediated by a causal SNP associated with both the tag SNP and
35 the trait. Nevertheless, it is difficult to determine the underlying causal variants due to complex patterns
36 of LD among SNPs. Moreover, quantitative trait locus (QTL) analyses have successfully identified variants
37 associated with molecular phenotypes i.e. gene expression, DNA methylation, chromatin accessibility [1, 2,
38 3, 4, 5]. These molecular QTL studies enable the understanding of molecular basis of GWAS SNPs via colo-
39 calization. However, the high sequencing cost leads to QTL studies with modest sample sizes, limiting the
40 power to uncover QTLs with small effects. Therefore, identification of these functional noncoding variants
41 that have direct functional consequence on complex traits and molecular phenotypes remains challenging
42 in human genetics research.

43 Several studies suggest that functional noncoding variants are believed to disrupt the normal regulatory
44 activity in promoter and enhancer regions in order to impact the downstream gene expression in a tissue or
45 cell type specific manner and thus result in the onset of disease such as the prevalence of TERT promoter
46 mutations has been established in melanoma, gliomas and bladder cancer [6]; novel MYB-binding motifs,
47 which are generated by somatic mutations in the intergenic regions, creates a super-enhancer upstream
48 of the TAL1 oncogene in a subset of T cell acute lymphoblastic leukaemia [7]. Moreover, more than 90% of
49 GWAS identified SNPs are noncoding and are enriched in regulatory elements (REs). A recent exploratory
50 study demonstrates that active chromatin marks (e.g. H3K27ac and H3K4me1), and repressive chromatin
51 marks (e.g. H3K9me3 and H3K27me3) show different regulatory activities between a risk variant rs3024505
52 associated with type 1 diabetes and a benign variant rs114490664 [8]. This example indicates that RE activity
53 can be used to distinguish the causal and non-causal SNPs.

54 The rapid development of massively parallel sequencing technologies enables the generation of thou-
55 sands of “multi-omics” data, which are publicly available at large national and international consortia such
56 as the Encyclopedia of DNA Elements (ENCODE) [9], Roadmap Epigenomics [10] and International Hu-

57 man Epigenome Consortium [11]. These multi-omics data measures genome-wide regulatory activities
58 such as histone modifications (e.g. ChIP-seq), methylation (e.g. methylation array, whole-genome bisulfite
59 sequencing), chromatin accessibility (e.g. DNase-seq, ATAC-seq) and chromatin interactions (e.g. Hi-C)
60 across hundreds of tissues and cell types. Using standard sequencing data processing protocols such as
61 peak-calling, tissue- or cell type-specific REs and RE activities can be detected. Variant annotations are
62 further created by overlapping variants and REs where the variant fall in [8, 12, 13, 14]. These annotations
63 have been widely used as predictive features to develop computational methods for predicting functional
64 noncoding variants [15, 16, 17, 18, 19, 20, 21], which adopt different computational methodologies, use dif-
65 ferent training variants and utilize different variant annotations. Among these methods, supervised learning
66 approaches, such as GWAVA [15], CADD [16], DANN [17], FATHMM-MKL [18]), LINSIGHT [19]), Fun-
67 Seq2 [20], are trained using labelled non-causal variants and causal ones, either putative or experimentally
68 validated, to predict the probability of a give variant for being causal. Different from the supervised learn-
69 ing methods, a common practice of unsupervised learning approaches such as Eigen [21] performs direct
70 aggregation of multi-dimensional variant annotations into one single functional score, which measures the
71 functional importance of the variant, without a training step. Importantly, for most of the existing meth-
72 ods, genome-wide precomputed functional scores for known variants from 1000 Genomes Project [22] or
73 gnomAD [23] are publicly available. Without the need to retrain the model, users can obtain these scores
74 efficiently by providing a list of variants identifiers or genomic coordinates and utilize these scores directly
75 for post-GWAS study i.e. fine mapping analysis. Usually, a larger score indicates the variant could poten-
76 tially be more functional and the variant with the highest score is prioritized in a risk locus with LD-linked
77 variants.

78 Nevertheless, without strong prior knowledge, it is difficult to choose which scoring method in real ap-
79 plication among multiple methods developed for the same purpose. It is even more challenging to make
80 the choice considering prediction performance of existing scoring methods has been shown poor concor-
81 dence on the state-of-the-art benchmark datasets [24]. There are two possible reasons to explain the poor
82 consistency. First, these methods are trained using different training variants and variant annotations to
83 predict functional noncoding variants from different context (i.e. disease, tissue or cell types), making one
84 method trained using variants from one context have suboptimal prediction for variants from another con-
85 text. Second, they adopt different algorithms tailored to specific scenarios, limiting the generality. For exam-

86 ple, GWAVA is developed using pathogenic regulatory variants from The Human Gene Mutation Database
87 (HGMD) [25] and is thus used to predict pathogenic regulatory variants; FunSeq2 is trained using recur-
88 rence cancer somatic variants and is therefore specifically designed to predict noncoding regulatory variants
89 in cancer. Considering the above challenge, given a variant without prior knowledge about its context and
90 functional consequence, an ensemble approach that combines the predictions of all these methods in a
91 weighted scheme could offer a more powerful prediction than each method. The weight of each individ-
92 ual scoring method, which reflects their contributions in the prediction task, can be adaptively learnt in
93 different context, which improves the generality and flexibility.

94 We hereby developed a statistical learning framework “WEVar” (Weighted Ensemble framework for
95 predicting functional regulatory Variants) by integrating representative scoring methods in a constrained
96 optimization approach, where the precomputed functional scores of these methods are treated as predictive
97 features with two constraints: i) the summation of weights of existing methods are required to be one; ii) a
98 L_2 -norm is further imposed on the weights for smoothing the weight estimation. There are several advan-
99 tages of WEVar. First, WEVar is developed directly on top of precomputed functional score, which is an
100 optimally integrative metric that represents for thousands of multi-omics functional annotations used by
101 each scoring method. Using these functional scores directly will decrease the number of predictive features
102 dramatically and thus avoid the challenge of high-dimensional data in the model development, that is, the
103 sample size of labelled causal variants is fewer than the number of variant annotations. Second, WEVar
104 leverages individual scoring method by adaptively learning the contribution of each one, which will up-
105 weight the methods fit more in the current context and down-weight the others, and thus optimizes the
106 prediction performance. Last but most importantly, WEVar has two modes: “context-free” and “context-
107 dependent”. Context-free WEVar is used to predict functional noncoding variants from unknown or het-
108 erogeneous context. Context-dependent WEVar can further improve the functional prediction when the
109 variants come from the same context in both training and testing set. Using simulation and real data stud-
110 ies, we demonstrate both WEVar modes outperform each individual scoring method on the state-of-the-art
111 benchmark datasets. Importantly, context-dependent WEVar can further improve the functional predic-
112 tion. We also show that WEVar can successfully prioritize experimentally validated regulatory variants
113 associated with different traits and located in different risk loci.

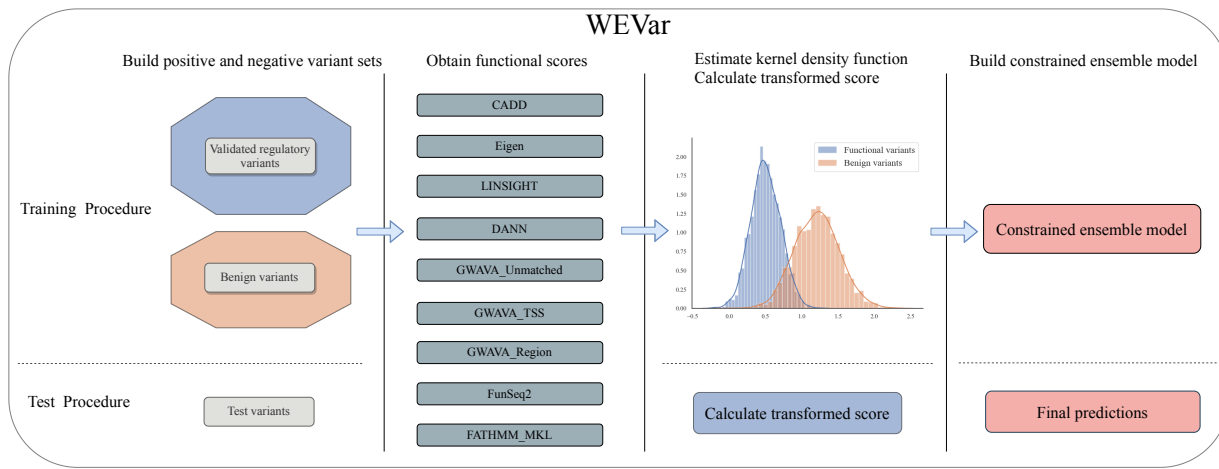


Figure 1. Overview of the WEVar. WEVar aims to predict functional noncoding variants, which has two modes: “context-free” and “context-dependent”. For “context-free” mode, the training variant set is chosen from a curated set of functional regulatory variants from diverse context to train a model for functional prediction of variants from unknown or heterogeneous context. For “Context-dependent” mode, the training variant set is selected from one specific context of interest (i.e. disease, tissue, cell type), to train a model for functional prediction of variants from the same context. In the training phase, WEVar compiles the training set with labelled functional and non-functional variants and annotate all variants with precomputed functional scores from representative scoring methods. For each method, the raw scores are transformed using kernel density function (KDE) for both functional and non-functional variant sets respectively. Using these transformed scores as predictive features, a constrained ensemble model is trained. In the testing phase, precomputed functional scores of testing variants are transformed based on the estimated KDE in the training phase and then serve as input features for trained ensemble model to predict the ensemble WEVar score.

114 **Results**

115 The overview of WEVar is shown in Figure 1. First, we will perform a simulation study to evaluate the accuracy of weight estimation by WEVar for all integrated scoring methods and investigate whether the prediction performance of WEVar is improved compared to individual scoring method. Second, we will evaluate the context-free functional prediction and context-dependent functional prediction on the state-of-the-art benchmark datasets respectively. Third, we will apply WEVar to prioritize experimentally validated causal regulatory variants in multiple risk loci associated with multiple traits.

121 **Evaluation of WEVar in a simulation study**

122 **Evaluation metrics**

123 The performance of all scoring methods is evaluated using area under the receiver operating characteristics curve (AUROC), the area under the precision-recall curve (AUPR) and Pearson correlation between pre-

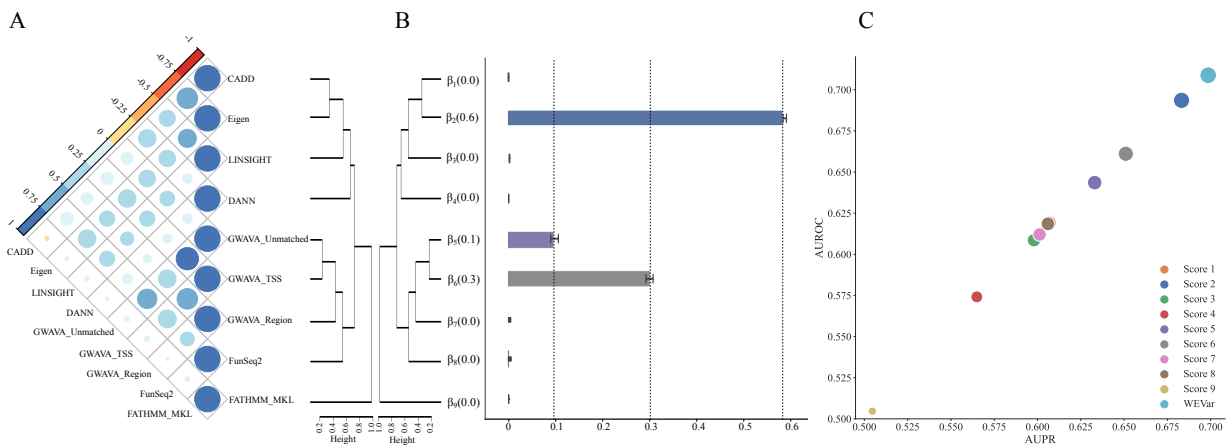


Figure 2. (A) Pairwise Pearson correlations between precomputed functional scores among scoring methods for the integrated causal regulatory variants collected from Li et al. [26]. (B) Average regression coefficient estimated by WEVar in the training phase in 50 simulations. (C) Average prediction performance by WEVar on the independent testing datasets. X axis presents AUPR; Y axis presents AUROC; the bubble size represents COR. AUPR, AUROC and COR are averaged in the testing phase in 50 simulations.

125 directed and true labels (COR). AUROC and AUPR are metrics based on the ranks of the predicted scores.
 126 COR has the additional ability to measure how the predicted values are correlated with the true labels. Using
 127 different probability cutoffs, AUROC measures the trade-off between the true positive rate and false positive rate.
 128 AUPR compares the trade-off between the true positive rate and precision. AUROC is preferred
 129 for balanced class, whereas AUPR is more appropriate for imbalanced class. Since we have both balanced
 130 and unbalanced testing datasets, we present both metrics.

131 Simulating correlated functional scores and variant labels

132 We conduct a simulation study to evaluate whether WEVar can estimate contribution of each individual
 133 scoring method accurately and whether WEVar can improve prediction performance compared to each
 134 individual scoring method. Since the functional scores of different methods have an overall positive correlation
 135 (Figure 2A), we simulate functional scores of all scoring methods with consideration of the score
 136 correlation. Using the simulated scores, we generate a total 10,000 variants with an equal size of functional
 137 and nonfunctional variants in the training set. Similarly, we independently generate an equal number of
 138 10,000 variants in the testing set for prediction evaluation. We then apply WEVar to retrain a model in the
 139 training set and predict WEVar scores in the testing set. Using WEVar scores and true labels in the testing
 140 set, we will calculate AUROC, AUPR and COR. We repeat the whole procedure 50 times and obtain the

141 average of all evaluation metrics.

142 Specifically, using the integrated causal regulatory variant set collected from Li et al. [26], we calculate
143 a $p \times p$ variance-covariance matrix R of precomputed functional scores among all integrated scoring meth-
144 ods, where p is the number of scoring methods. We cluster these methods based on Pearson correlation and
145 find that these methods have different levels of disagreement, indicating that performance of these meth-
146 ods show poor concordance on the benchmark dataset (Figure 2A). Not surprisingly, GWAVA_Unmatched,
147 GWAVA_Region and GWAVA_TSS are clustered together since they use the same positive training variant
148 set. Surprisingly, FATHMM-MKL has the lowest correlation with all the other methods. Indeed, this obser-
149 vation highlights the rationale why a weighted ensemble strategy proposed by WEVar is essential to improve
150 the prediction because it is able to upweight the scoring methods fit in current context while down-weight
151 the unfit others. We further perform Cholesky decomposition on R as:

152
$$R = C \cdot C^\top \quad (1)$$

153 where C is a $p \times p$ lower triangular matrix with real positive diagonal entries. To maintain the correlations
154 of simulated scores, we generate the correlated functional scores X as the product between C^\top and random
155 variable d , which is sampled from an independent normal distribution as:

156
$$X = d \cdot C^\top, \quad d \sim N(0, 1). \quad (2)$$

157 where x_{ij} as the functional score of i th noncoding variant in j th scoring method. η_i , which is the weighted
158 average score of i th variant, can be generated as:

159
$$\eta_i = \sum_{j=1}^p x_{ij} \cdot \beta_j \quad (3)$$

160 where β_j is the weight associated with j th method. Without loss of generality, we manually assign 0.6 to
161 β_2 , 0.3 to β_6 , 0.1 to β_5 , and 0 to the rest. We then perform inverse logit transformation to η_i to obtain
162 probability π_i , based on which the binary label y_i for i th variant is generated from a Bernoulli distribution
163 as:

164
$$y_i \sim \text{Bern}(\pi_i), \quad \text{where } \pi_i = \frac{e^{\eta_i}}{1 + e^{\eta_i}}. \quad (4)$$

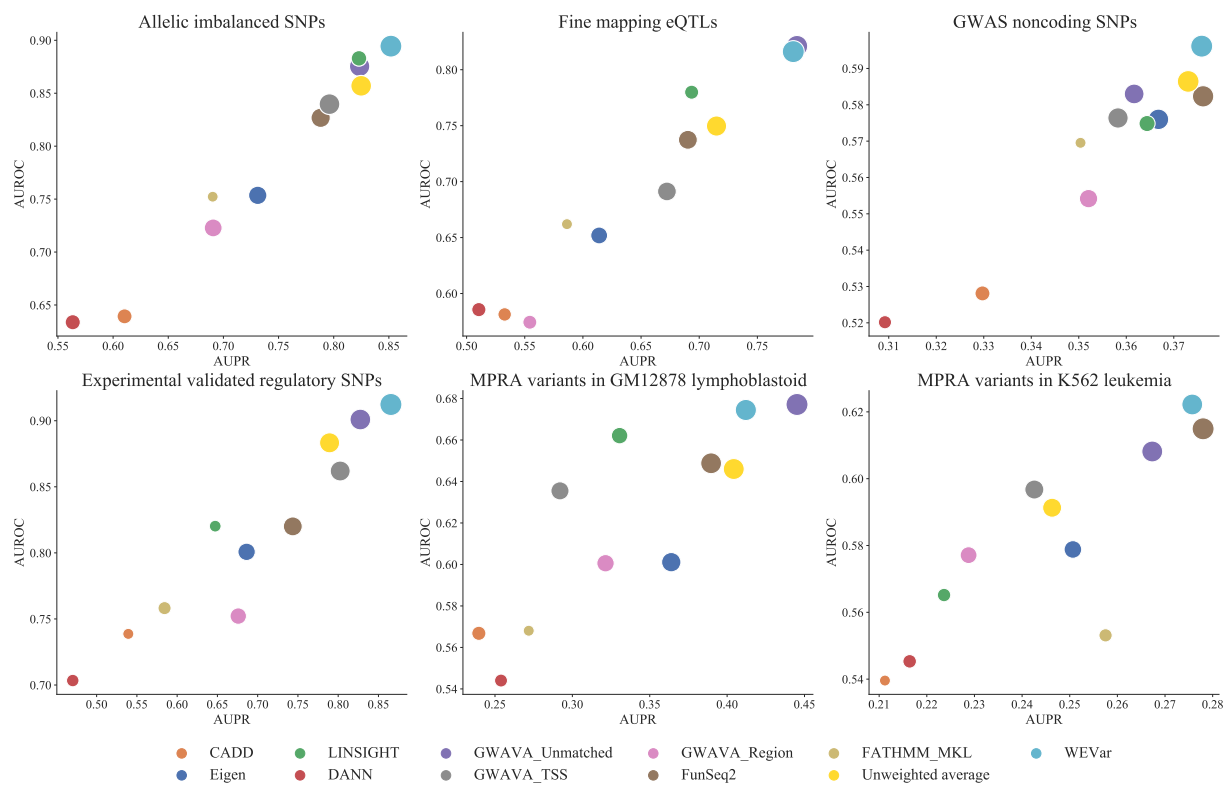


Figure 3. Evaluation of context-free WEVar and integrated scoring methods. Context-free WEVar is trained using the integrated functional regulatory variants collected by Li et al. [26], which include variants in HGMD, ClinVar, OregAnno and fine-mapping candidate causal SNPs for 39 immune and non-immune diseases with a total of 5,247 positive variants and 55,923 negative variants. Context-free WEVar is tested on the state-of-the-art benchmark datasets, which include i) Allelic imbalanced SNPs in chromatin accessibility with a total of 8,592 positive variants and 9,678 negative variants (Allelic imbalanced SNPs); ii) Uniformly processed fine-mapping eQTLs from 11 studies with a total of 31,118 positive variants and 36,540 negative variants (Fine mapping eQTLs); iii) GWAS noncoding SNPs with a total of 19,797 positive variants and twice number of negative variants (GWAS SNPs) [27]; iv) Manually curated experimentally validated regulatory SNPs with a total of 76 positive variants and 156 negative variants (Experimentally validated regulatory SNPs); v) MPRA validated variants in lymphoblastoid cells with a total of 693 positive variants and 2,772 negative variants (MPRA variants in GM12878 lymphoblastoid); vi) MPRA validated variants in erythrocytic leukemia cells with a total of 342 positive variants and 1,368 negative variants (MPRA variants in K562 leukemia). We further remove variants on sex chromosome or with missing precomputed scores. X axis presents AUPR; Y axis presents AUROC; the bubble size represents COR.

165 Results of the simulation study

166 In the simulation study, we will evaluate whether WEVar can truly discover the contributions of individual
 167 scoring method by comparing the estimated regression coefficients ($\hat{\beta}$) with the assigned true values (β).
 168 To fit a WEVar model, the optimal tuning parameter for L_2 -norm is selected using fivefold cross-validation
 169 (5-CV), where the whole training set is divided into five-folds, where four-folds is used to train the model
 170 and one-fold is used to obtain the evaluation metric i.e. AUROC. The optimal tuning parameter is chosen

¹⁷¹ based on the average AUROC from 5-CV, and a final model is fitted using the whole training set with the
¹⁷² optimal tuning parameter. To evaluate the performance of the final model an independent testing set, we
¹⁷³ use all evaluation metrics AUROC, AUPR and COR.

¹⁷⁴ As a result, we find that the estimated weights are nearly unbiased to the underlying truths (Figure 2B),
¹⁷⁵ which suggests that WEVar can discover the contribution of each individual scoring method correctly when
¹⁷⁶ the functional scores of these methods are correlated. With accurate contribution estimation, WEVar can
¹⁷⁷ significantly improve the prediction performance in the independent testing (Figure 2C) by achieving the
¹⁷⁸ highest AUROC, AUPR and COR. Overall, the simulation results validate the benefit of exploiting different
¹⁷⁹ scoring methods in an integrative weighted scheme.

¹⁸⁰ **Context-free functional prediction**

¹⁸¹ **Overview of context-free WEVar**

¹⁸² We first introduce context-free WEVar, which is trained using integrated causal regulatory variants col-
¹⁸³ lected from Li et al. [26]. We call this WEVar mode “context-free” because these variants are not limited
¹⁸⁴ to a specific context but have a broad definition of functionality across a wide range of context. These vari-
¹⁸⁵ ants are either experimentally validated or highly putative causal variants associated with different diseases,
¹⁸⁶ molecular phenotypes or clinical outcomes, which are located in different noncoding regions such as pro-
¹⁸⁷ moters, enhancers, 5'UTRs and 3'UTRs. The diverse context and widespread genomic locations of these
¹⁸⁸ variants make it potentially powerful to predict functional noncoding variants when the context is unknown
¹⁸⁹ or heterogeneous. To demonstrate the generality of context-free WEVar, we evaluate it on the independent
¹⁹⁰ benchmark datasets containing noncoding variants of different functionalities and from diverse context.
¹⁹¹ We also remove any duplicated variants overlapped with training dataset from each independent testing
¹⁹² dataset, which can prevent potential overfitting. To verify the effectiveness of the weight strategy, besides
¹⁹³ all scoring methods WEVar integrates, we also include “Unweighted average” as a comparison, which is the
¹⁹⁴ unweighted average of min-max normalized precomputed functional scores from the integrated methods.
¹⁹⁵ In the training phase of WEVar, tuning parameter for L_2 -norm is selected using 5-CV. For all methods,
¹⁹⁶ AURPC, AUCPR and COR are reported on each independent testing dataset.

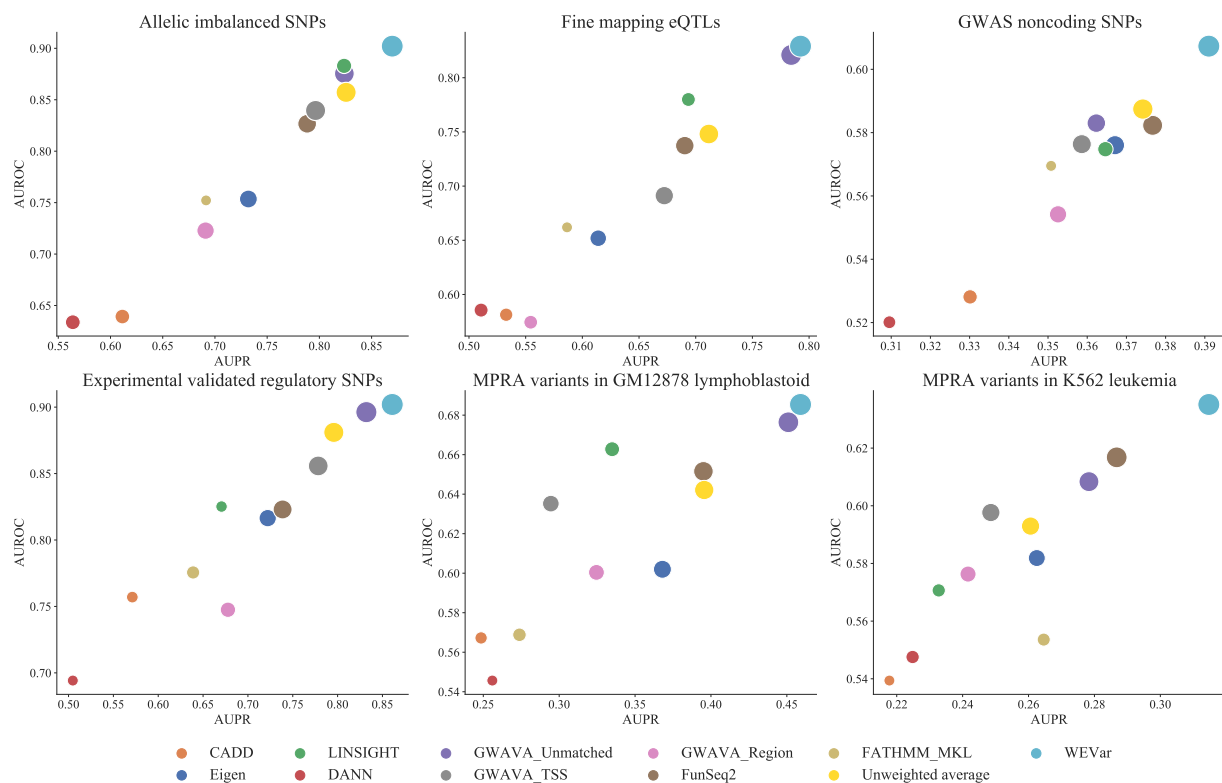


Figure 4. Evaluation of context-dependent WEVar and integrated scoring methods on state-of-the-art benchmark datasets, which include Allelic imbalanced SNPs, Fine mapping eQTLs, GWAS noncoding SNPs, Experimentally validated SNPs, MPRA validated variants in GM12878 lymphoblastoid cells and MPRA validated variants in K562 leukemia cells. We further remove variants on sex chromosome or with missing precomputed scores. To restrict the training and testing variants are from the same context, for each dataset, we randomly split the dataset into ten-folds with nine-folds as the training set and one-fold as the testing set. Context-dependent WEVar is trained on the nine-folds and independently evaluated on the left one-fold. AUC, AUCPR and COR are calculated and averaged in the ten replicates for each method. X axis presents AUPR; Y axis presents AUROC; the bubble size represents COR.

197 Results of functional prediction between context-free WEVar and integrated scoring methods

198 We start to compare the prediction performance between WEVar and its integrated scoring methods on
 199 three datasets, which consist of putatively functional variants based on statistical association (Figure 3).
 200 The first dataset, which is produced by Maurano et al. [28] and processed by Li et al. [26], contains
 201 8,592 significant allelic imbalanced SNPs of chromatin accessibility (FDR<0.1) as the positive set and 9,678
 202 frequency-matched background SNPs around nearest transcription start sites of randomly selected genes as
 203 the negative set. We observe that WEVar obtains the largest AUROC, AUPR and COR (0.894, 0.852, 0.644)
 204 with substantial improvements over each individual scoring method (Table S1). Following WEVar, LIN-
 205 SIGHT, GWAVA_Unmatched and Unweighted average have an overall comparable performance. However,

206 the COR of LINSIGHT is much lower (0.255) compared to GWAva_Unmatched (0.535) and Unweighted
207 average (0.559). Surprisingly, FATHMM_MKL also has the lowest COR (0.053). Moreover, CADD and
208 DANN, which utilize the same training set, have comparable but poorest performance among all meth-
209 ods (CADD: 0.639, 0.610, 0.228; DANN: 0.634, 0.563, 0.236). Interestingly, the prediction performance of
210 GWAva_Unmatched, GWAva_TSS and GWAva_Region are discordant even if they use the same positive
211 training set (GWAva_Unmatched: 0.875, 0.823, 0.535; GWAva_TSS: 0.840, 0.796 0.559; GWAva_Region:
212 0.723, 0.691, 0.382).

213 The second dataset consists of eQTLs in 11 studies across 7 tissues identified from Brown et al. [29] and
214 processed by Li et al. [26]. The positive set consists of 31,118 significant eQTL SNPs (FDR<0.1) and the
215 negative set contains 36,540 frequency-matched background SNPs around nearest TSS of randomly selected
216 genes. We observe that WEVar has the largest COR and comparable AUROC and AUPR to GWAva_Un-
217 matched (WEVar: 0.816, 0.781, 0.509; GWAva_Unmatched: 0.821, 0.781, 0.476) (Table S2). Moreover,
218 both WEVar and GWAva_Unmatched have clearly advantages over other scoring methods. For example,
219 they improve nearly 0.04 AUROC and 0.09 AUPR over LINSIGHT, and 0.07 AUROC and 0.07 AUPR over
220 Unweighted average. Particularly, there is substantial improvement of nearly 0.1 COR to Unweighted av-
221 erage and over 0.3 to LINSIGHT. Notably, the relative performance of GWAva_Region drops dramatically
222 and it has the lowest AUROC (0.574). FATHMM_MKL still has the lowest COR (0.047) followed by CADD
223 and DANN (0.126, 0.1500).

224 The third dataset collects 19,797 GWAS significant noncoding SNPs from NHGRI-EBI GWAS Catalog
225 [30] as positive set and twice number of variants in the negative set, which are randomly sampled from all
226 noncoding variants in 1000 Genomes project with minor allele frequency (MAF) $\geq 5\%$ [27]. The relative
227 prediction performance of all methods are similar to the first dataset of allelic imbalanced SNPs. WEVar
228 outperforms all scoring methods by obtaining the highest AUROC, AUPR, and COR. FATHMM_MKL
229 have the lowest COR, while CADD and DANN have the lowest AUROC and AUPR (Table S3).

230 In addition to the three datasets comprised of putatively functional noncoding variants derived from
231 association analyses, we compare the prediction performance between WEVar and all scoring methods on
232 three datasets consisting of experimentally validated regulatory variants. The first dataset include 81 exper-
233 imentally validated regulatory SNPs curated by Li et al. [26]. We find the trends of prediction performance
234 for all methods still holds similarly to allelic imbalanced SNPs and GWAS significant noncoding SNPs,

²³⁵ where WEVar obtains the largest AUROC, AUPR and COR (0.912, 0.865, 0.718) followed by GWAU_Un-
²³⁶ matched (0.901, 0.828, 0.649) and Unweighted average (0.883, 0.789, 0.617) (Table S4).

²³⁷ The other two datasets contain processed causal regulatory variants validated by MPRA in two cell
²³⁸ lines [31]. The first MPRA dataset includes 665 variants with genomic loci annotation in Ensembl database
²³⁹ as positive set, which are selected out of 842 expression-modulating variants that show significantly dif-
²⁴⁰ ferential allelic expression in GM12878 lymphoblastoid cells [32]. The negative set contains 2,772 control
²⁴¹ variants tested by MPRA but neither allele showed significant effects on expression (Bonferroni corrected
²⁴² pvalue > 0.1). The second MPRA dataset consists of 339 positive variants that cause significant change of
²⁴³ expression via targeted motif disruption in enhancers in K562 erythrocytic leukemia cells (pvalues < 0.05)
²⁴⁴ [33]. The negative set contains 1,359 control variants without causing significant change (pvalues > 0.1).
²⁴⁵ As a result, WEVar has comparable performance with top-performed GWAU_Unmatched in predict-
²⁴⁶ ing MPRA validated regulatory variants in GM12878 lymphoblastoid cells (WEVar: 0.674, 0.412, 0.286
²⁴⁷ vs GWAU_Unmatched: 0.677, 0.445, 0.317) (Table S5). WEVar achieves largest AUROC and AUPR in
²⁴⁸ predicting MPRA validated regulatory variants in K562 leukemia cells (Table S6).

²⁴⁹ Clearly, context-free WEVar has the overall best performance on the state-of-the-art independent test-
²⁵⁰ ing datasets, which demonstrate its robustness and generality to predict functional noncoding variants
²⁵¹ across a wide range of context. Following WEVar, GWAU_Unmatched, Unweighted average and FunSeq2
²⁵² have superior performance to others. In contrast, CADD, DANN and FATHMM_MKL perform poorly.
²⁵³ Particularly, FATHMM_MKL suffers from a low COR. Notably, integrating scores in a weighted scheme in-
²⁵⁴ deed boosts the prediction performance as demonstrated by the improvement of WEVar over Unweighted
²⁵⁵ average.

²⁵⁶ Context-dependent functional prediction

²⁵⁷ Overview of context-dependent WEVar

²⁵⁸ Different from context-free functional prediction, context-dependent functional prediction happens when
²⁵⁹ a context-dependent WEVar is trained and the training and testing variants are from the same context.
²⁶⁰ We develop “context-dependent” mode for WEVar because functional variants are usually studied in a cell
²⁶¹ type/tissue-specific way. The context-matching between training and testing variants may improve the pre-
²⁶² diction power. We demonstrate the prediction performance of context-free WEVar first, followed by a

²⁶³ comparison between context-free and context-dependent WEVar to demonstrate the advantage for WEVar
²⁶⁴ by being context-dependent.

²⁶⁵ **Results of functional prediction between context-dependent WEVar and integrated scoring methods**

²⁶⁶ We use the same benchmark datasets to evaluate context-free functional prediction. To restrict the training
²⁶⁷ and testing variants from the same context, we randomly split each dataset into ten-folds with nine-folds
²⁶⁸ as the training set and one-fold as the testing set. Tuning parameter for L_2 -norm is selected in the training
²⁶⁹ set using 5-CV with AUROC as the evaluation metric. A final context-dependent WEVar is fitted using the
²⁷⁰ whole training set with the selected tuning parameter and makes the functional prediction on the testing
²⁷¹ set. AUROC, AUPR and COR are calculated by comparing prediction scores and true labels of variants in
²⁷² the testing set. We use leave-one-fold-out by selecting nine-folds as training set and one-fold as testing set
²⁷³ ten times. Accordingly, the whole procedure is repeated ten times and all evaluation metrics are reported
²⁷⁴ as average.

²⁷⁵ We observe that context-dependent WEVar outperforms all scoring methods by obtaining the highest
²⁷⁶ AUROC, AUPR and COR across all the benchmark datasets (Figure 4 and Table S1-S6). Moreover, we
²⁷⁷ observe similar trends between context-dependent and context-free functional prediction, where WEVar,
²⁷⁸ GWAVA_Unmatched and Unweighted average are the top-performed methods, while CADD, DANN and
²⁷⁹ FATHMM_MKL have overall poor performance.

²⁸⁰ To further objectively gauge the performance of context-dependent WEVar, we utilize the training and
²⁸¹ testing variant set in the first part of challenge of Critical Assessment of Genome Interpretation eQTL chal-
²⁸² lenge (CAGI) [34] derived from MPRA validated regulatory variants from GM12878 lymphoblastoid cells
²⁸³ [32]. The variants selected by CAGI show significant level of transcriptional activity for either of two alleles.
²⁸⁴ Specifically, the level of transcriptional activity is measured by differential abundance of transcripts versus
²⁸⁵ plasmid input. Based on the FDR cutoff 0.01, a binary label is generated to indicate whether or not at least
²⁸⁶ one of the two alleles of the variant exhibits a significantly high transcriptional activity (i.e. labeling 1 if
²⁸⁷ FDR<0.01, otherwise, 0). As a result, the training set consists a total of 2,873 SNVs with 345 as positive set
²⁸⁸ and 2,528 as negative set. The testing set contains a total of 2,808 SNVs with 348 positive variants and 2,460
²⁸⁹ negative variants. We further remove SNVs on sex chromosome or with missing precomputed scores in
²⁹⁰ both sets. Besides following the original training and testing procedure, we further carry out an additional

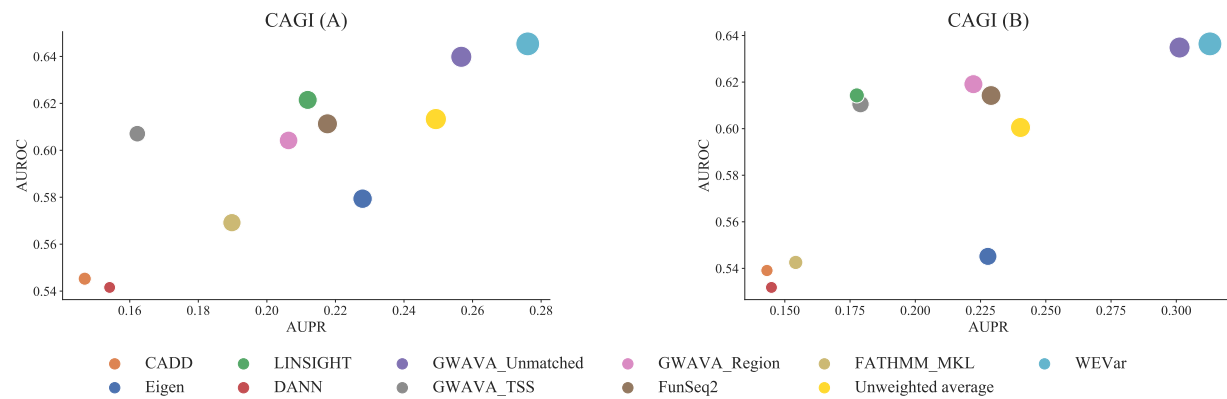


Figure 5. Prediction performance comparison between context-dependent WEVar and integrated scoring methods on the CAGI benchmark datasets. In CAGI, 2,873 SNVs with 345 as positive set and 2,528 as negative set. The testing set contains a total of 2,808 SNVs with 348 positive variants and 2,460 negative variants. We further remove SNVs on sex chromosome or with missing precomputed scores in both sets. (A) Context-dependent WEVar is first trained on the training set and evaluated on the testing set. (B) Similarly, we switch the training and testing set and perform an additional independent evaluation. The figure presents the AUPR, AUROC, and COR. X axis presents AUPR; Y axis presents AUROC; bubble size represents COR.

291 comparison by switching the training and testing set.

292 Consistent with our previous findings, context-dependent WEVar has superior performance to other
 293 scoring methods in both comparisons by achieving the highest AUROC, AUPR and COR, followed by
 294 GWAVA_Unmatched and Unweighted average (Figure 5, Table S7-8). Moreover, CADD and DANN have
 295 the overall poorest performance. The additional independent evaluation further strengthens the advan-
 296 tage of context-dependent WEVar in predicting functional noncoding variants by benefiting from matched
 297 context in training and testing set.

298 Besides improving the functional prediction, another important characteristic of WEVar is that it can
 299 identify the informative predictors that play the major contribution to the functional prediction among all
 300 integrated scoring methods. Consequently, we find that sets of informative predictors are different across
 301 benchmark datasets (Figure S1, Table S9). In most cases, WEVar identifies a parsimonious set of scoring
 302 methods that dominate the functional prediction especially FunSeq2 and GWAVA_Unmatched are two
 303 ubiquitous major contributors. Moreover, GWAVA_TSS is an additional major contributor for Allele im-
 304 balanced SNPs, Experimentally validated regulatory SNPs and integrated causal regulatory variants used
 305 by context-free WEVar. Regarding MPRA validated regulatory variants in GM12878 lymphoblastoid cells,
 306 Eigen is the additional method that has a major contribution. Similarly, GWAVA_Region and Eigen are two

307 additional major contributors for two comparisons for CAGI training and testing variants. However, for
308 GWAS noncoding SNPs and MPRA validated regulatory variants in K562 leukemia cells, there is a ubiq-
309 uitous solution, where the contributions of all methods are relative uniform. These findings demonstrate
310 that considering context-specificity in WEVar leads to different weight estimates and result in different
311 sets of informative predictors. These observations also suggest that it is important to obtain an optimal
312 weights when integrating different scoring methods, as the non-uniform weights estimated by WEVar lead
313 to improved functional prediction across benchmark datasets. Additionally, this point has been validated by
314 both simulation and real data applications that WEVar outperforms the Unweighted average.

315 **Results of comparison between context-free and context-dependent functional prediction**

316 We hypothesize that considering context-specificity and context-matching context between training and
317 testing variants in “context-dependent” WEVar will likely improve the predictive power for functional pre-
318 diction. To validate this hypothesis, we directly compare the results of functional predictions between
319 context-free and context-dependent WEVar on the aforementioned state-of-the-art benchmarking datasets
320 (Figure S2, Table S1-S6).

321 For MPRA validated variants in GM12878 lymphoblastoid cells, context-dependent WEVar signifi-
322 cantly outperforms context-free WEVar with large performance gain in around 5% AUPR and 8% COR
323 but modest gain in AUROC. Similarly, context-dependent WEVar also achieves a large improvement by
324 increasing about 4% AUPR and 4% COR but slightly improvement of AUROC for MPRA validated variants
325 in K562 leukemia cells. Moreover, the improvement of context-dependent WEVar is evident demonstrated
326 by nearly 5% and 3% increase in COR but slightly increase in AUROC and AUPR for both Fine mapping
327 eQTLs and Allele imbalanced SNPs. In addition, context-dependent WEVar has a modest improvement of
328 all metrics for GWAS noncoding SNPs. However, there is a lack of improvement on Experimentally vali-
329 dated regulatory SNPs, which could be explained by the small sample size of training set. This observation
330 indicates that a large training set is necessary to improve the predictive power for context-dependent func-
331 tional prediction. Overall, the comparisons between context-dependent and context-free WEVar validate
332 the hypothesize that considering context-specificity and context-matching will improve the functional pre-
333 diction. However, this improvement depends on the availability of enough sample size for training a robust
334 context-dependent WEVar.

335 Prioritization of causal regulatory variants by WEVar on benchmarking datasets

336 To demonstrate the application of WEVar in studying complex traits, we apply genome-wide functional
337 scores of all noncoding variants in 1000 Genomes Project precomputed by context-free WEVar for fine-
338 mapping analysis in risk loci. The diverse benchmarking datasets are generated from different experiments
339 and study different traits, which are able to test the robustness of WEVar in prioritizing causal regulatory
340 variants in risk loci.

341 Noncoding variants modulating gene expression

342 We evaluate WEVar on reported “expression-modulating variants” (emVars), which have been validated to
343 show differential gene expression between alleles, from the MPRA study in GM12878 lymphoblastoid cells
344 [32]. To assess whether these emVars with a strong linkage to GWAS SNPs can be prioritized by WEVar
345 score, we create an extended LD block ($r^2 > 0.2$) utilizing ldproxy [35] to extract variants from all reference
346 populations within the LD block, which are further assigned WEVar score.

347 Consequently, WEVar is able to prioritize emVars in example LD blocks (Figure S3 and Table S10).
348 For example, emVar rs4790718 (chr17:4870893) scores higher than three LD-linked GWAS SNPs rs1060431
349 (chr17:4840868, $pvalue=2 \times 10^{-26}$), rs6065 (chr17:4836381, $pvalue=2 \times 10^{-12}$) and rs571461910 (chr17:4869143,
350 $pvalue=3.98 \times 10^{-9}$), which are mapped to SPAG7 and associated with Platelet counts. Similarly, em-
351 Var rs922483 (chr8:11351912) is successfully prioritized by the highest score among all LD-linked variants
352 including GWAS SNP rs2736340 (chr8:11343973, $pvalue=6.03 \times 10^{-20}$) associated with Systemic lupus
353 erythematosus. Moreover, emVar rs56316188 (chr8:59323811) scores higher than GWAS SNP rs2859998
354 (chr8:59324162, $pvalue=1 \times 10^{-7}$), which is mapped to UBXN2B and associated with narcolepsy with cat-
355 aplexy. Additionally, emVar rs306587 (chr10:30722908) is prioritized among LD-linked variants including
356 one GWAS SNP rs1042058 (chr10:30728101, $pvalue=6 \times 10^{-11}$). Overall, these examples demonstrate that
357 WEVar can successfully prioritize experimentally validated regulatory variants that modulate gene expres-
358 sion among LD-linked putatively causal GWAS SNPs, indicating that WEVar can potentially aid the fine
359 mapping analysis.

360 Causal regulatory variants associated with Schizophrenia

361 Schizophrenia, typically diagnosed in the late teens years to early thirties, is a mental disorder character-
362 ized by disruptions in thought processes, perceptions, emotional responsiveness, and social interactions.
363 Schizophrenia is one of the top 15 leading causes of disability worldwide [36, 37] and estimated interna-
364 tional prevalence of schizophrenia among non-institutionalized persons is 0.33% to 0.75% [38]. Although
365 GWAS has identified numerous noncoding schizophrenia-associated variants hypothesized to affect gene
366 transcription, the causal regulatory variants are still elusive. To experimentally evaluate the regulatory po-
367 tential of these GWAS SNPs and LD-linked variants, a recent study [39] screens several schizophrenia loci
368 from a large GWAS cohort-Schizophrenia Working Group of the Psychiatric Genomics Consortium, using
369 MPRA experiments in both K562 leukemia cells and SK-SY5Y neuroblastoma cells.

370 We apply context-free WEVar functional scores to discover causal regulatory variants associated with
371 Schizophrenia. Briefly, we define “causal regulatory variants” as variants with significant differential expres-
372 sion between two alleles with a FDR cutoff 0.2. For each causal regulatory variant, we extend the risk locus
373 by considering all variants in LD ($r^2 > 0.2$). We further obtain precomputed context-free WEVar score
374 for all variants in the risk locus. As a result, WEVar successfully prioritizes causal regulatory variants in the
375 risk loci by assigning them the highest WEVar score (Figure 6 and Table S11). For example, rs34877519
376 (chr3:2554612) is successfully prioritized by obtaining the score higher than any variant in the risk locus
377 including GWAS SNPs rs11708578 (chr3:2515894, pvalue=7.08 $\times 10^{-11}$) and rs17194490 (chr3:2547786,
378 pvalue=1.00 $\times 10^{-11}$); rs7927437 (chr11:123395987) receives the highest score among all variants in the risk
379 locus including GWAS SNP rs77502336 (chr11:123394636, pvalue=3.98 $\times 10^{-10}$); rs7779548 (chr7:137074540)
380 scores higher than any variant in the risk locus including GWAS SNP rs3735025 (chr7:137074844, pvalue=3.98 \times
381 10 $\times 10^{-12}$); rs6498914 (chr16:63699425) obtains the highest score among all variants in the risk locus including
382 GWAS SNP rs2018916 (chr16:63700508, pvalue=7.08 $\times 10^{-9}$). Overall, these findings demonstrates that
383 causal regulatory variants are not necessary the GWAS lead SNPs but the LD-linked variants. In addition,
384 WEVar is a powerful tool in post-GWAS analysis to pinpoint the causal regulatory variants in the risk loci,
385 which cannot be identified by a standard GWAS approach.

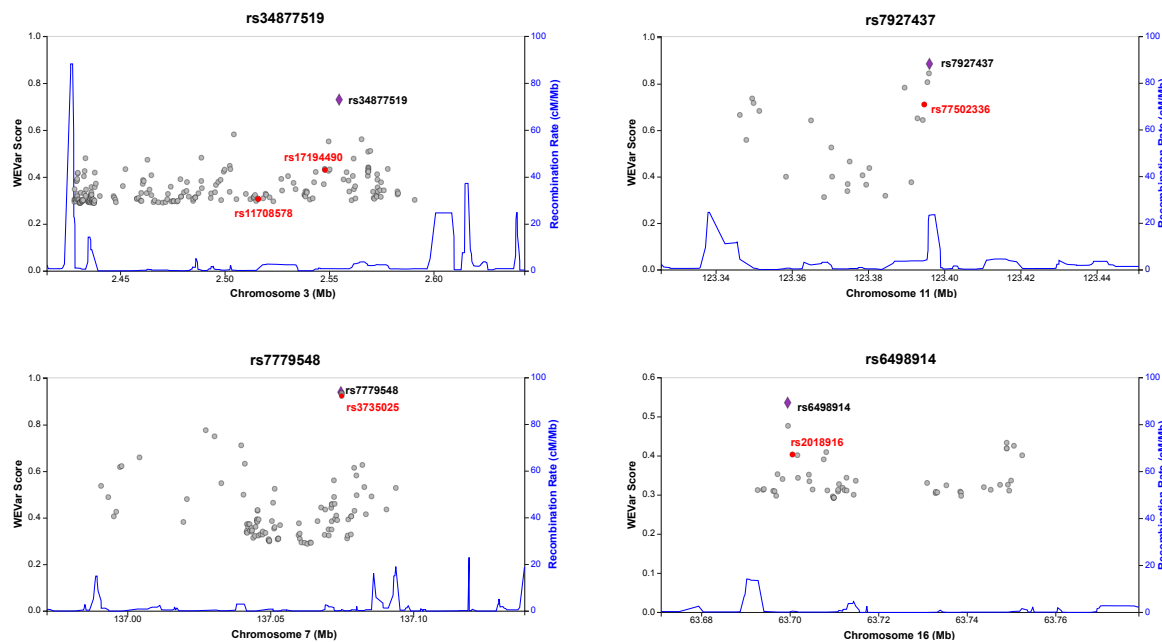


Figure 6. WEVar can prioritize causal regulatory variants associated with Schizophrenia. Causal regulatory variants are defined as variants with significant differential expression between two alleles ($FDR < 0.2$) in MPRA experiments in both K562 leukemia cells and SK-SY5Y neuroblastoma cells. For each causal regulatory variant, we extend the risk locus by considering all variants in LD ($r^2 > 0.2$). As a result, rs34877519 (chr3:2554612) is successfully prioritized by obtaining the score higher than any variant in the risk locus including GWAS SNPs rs11708578 (chr3:2515894, $pvalue=7.08 \times 10^{-11}$) and rs17194490 (chr3:2547786, $pvalue=1.00 \times 10^{-11}$); rs7927437 (chr11:123395987) receives the highest score among all variants in the risk locus including GWAS SNP rs77502336 (chr11:123394636, $pvalue=3.98 \times 10^{-10}$); rs7779548 (chr7:137074540) scores higher than any variant in the risk locus including GWAS SNP rs3735025 (chr7:137074844, $pvalue=3.98 \times 10^{-12}$); rs6498914 (chr16:63699425) achieves the highest score among all variants in the risk locus including GWAS SNP rs2018916 (chr16:63700508, $pvalue=7.08 \times 10^{-9}$). The causal regulatory variants validated by MPRA are marked purple. LD-linked GWAS SNPs are marked red.

386 Causal regulatory variants associated with multiple traits and validated by multiple platforms

387 We benchmark WEVar on state-of-the-art datasets, which are generated from multiple studies for different
388 traits such as Cleft lip/palate, heart, hair color and breast cancer and consists of regulatory variants exper-
389 imentally validated by different functional assays. Similar to previous analyses, we define the risk locus
390 by considering all variants in LD ($r^2 > 0.2$) for each regulatory variant. Consequently, WEVar is able to
391 prioritize regulatory variants in each risk locus (Figure S4 and Table S12).

392 Specifically, rs6801957 (chr3:38767315, $pvalue=9 \times 10^{-9}$), located in intronic region of SCN10A, has
393 been validated by BAC reporter system and 4C-seq to modulate cardiac SCN5A expression [40]. Consistent
394 with the experimental validation, WEVar assigns the highest score to rs6801957 in the risk locus, which also
395 includes multiple GWAS SNPs rs6795970 (chr3:38766675, $pvalue=1 \times 10^{-58}$), rs7433306 (chr3:38770639,

396 pvalue=1 × 10⁻¹⁴), rs6790396 (chr3:38771925, pvalue=2 × 10⁻³⁹), rs6599255 (chr3:38796415, pvalue=2 ×
397 10⁻¹⁰) rs6798015 (chr3:38798836, pvalue=2 × 10⁻¹²) and rs10428132 (chr3:38777554, pvalue=1 × 10⁻⁶⁸).
398 We further evaluate another variant rs227727 (chr17:54776955, pvalue=7.3 × 10⁻⁸), which is mapped to
399 17q22 NOG locus and found associated with Cleft lip/palate. The NSCL/P-associated allele of rs227727
400 significantly decreases the nearby enhancer activity compared to the unassociated allele, which is experi-
401 mentally validated by quantitative reporter assays transfected with a luciferase reporter vector [41]. Sim-
402 ilarly, rs227727 is prioritized with the highest score in the risk locus. The next evaluated variant rs12821256
403 (chr12:89328335, pvalue=4 × 10⁻³⁰) is located in a regulatory enhancer in the upstream of lncRNA LINCo2458.
404 It has been experimentally validated that rs12821256 is associated with hair color by altering the binding
405 site of lymphoid enhancer-binding factor1 (LEF1) transcription factor. The altered binding site of LEF will
406 reduce LEF responsiveness and enhancer activity in cultured human keratinocytes [42]. Again, rs12821256
407 scores highest in the risk locus, which is supported by the experimental finding. The last investigated vari-
408 ant is a breast cancer risk SNP rs11055880 (chr12:14410734), which resides in an intergenic enhancer and
409 validated by CRISPR-Cas9 approach [43] to have endogenous regulatory activities on expression of ATF7IP.
410 Consistently, rs11055880 obtains the highest score among all variants in the risk locus.

411 Overall, the consistency between experimental validations and prioritization results based on WEVar
412 score demonstrates the capability and robustness of WEVar to prioritize functional noncoding variants in a
413 LD-linked risk locus. The robustness is reflected by the successful prioritization of heterogeneous variants,
414 which are located in various genomic regions, associated with different traits, and validated by different
415 functional assays.

416 Discussion

417 In this work, we develop a statistical learning framework “WEVar” to predict functional noncoding vari-
418 ants by integrating representative scoring methods in an optimized weighted scheme. The development of
419 WEVar is motivated by the existing gap of strong discordant performance of existing methods on state-of-
420 the-art benchmark datasets, as shown by the inconsistent prediction performance of these methods on the
421 integrated causal regulatory SNPs (Figure 2A).

422 Overall, the advantages of WEVar lies on several aspects. First, existing approaches, either supervised
423 or unsupervised, are developed using thousands of functional annotations derived from multi-omics data

424 deposited in large national consortia such as ENCODE and Roadmap Epigenomics. Different from exist-
425 ing methods, WEVar is developed on top of these methods by directly utilizing genome-wide precomputed
426 functional scores, which collapse multi-dimensional functional annotations into a single score. Therefore,
427 without losing information of functional annotations, direct application of the functional scores of exist-
428 ing approaches significantly reduces the dimensionality of feature space in model development of WEVar.
429 Second, WEVar will identify informative predictors in an optimized weighted scheme and thus can lever-
430 age the advantages of different approaches, which likely lead to improved prediction performance com-
431 pared to each integrated individual scoring method. Third, WEVar offers two modes: “context-free” and
432 “context-dependent”. Each mode has its favorite scenario. We adopt a comprehensive training set [26],
433 which integrates curated causal SNPs, located in different genomic regions, collected from different sources
434 and associated with different traits to develop context-free WEVar. The large sample size, diverse context
435 and genomic locations as well as heterogeneous trait association of these training variants make context-
436 free WEVar powerful to predict functional noncoding variants with unknown or heterogeneous context. In
437 contrast, training variant set of context-dependent WEVar is derived from the same context i.e. tissue-, cell
438 type-, disease-specific. The context-specificity of training set makes context-dependent WEVar prefer the
439 scenario when noncoding variants in training and testing set are from the same context, which may lead to
440 improvement of functional prediction.

441 We perform a real data-based simulation study by considering the inherent correlations of precomputed
442 functional scores among integrated scoring methods. The results demonstrate that WEVar outperforms
443 individual scoring method and can estimate the contributions of integrated scoring methods accurately,
444 which may explain the improved performance of WEVar. Next, we evaluate context-free functional pre-
445 diction and context-dependent functional prediction respectively on state-of-the-art benchmark datasets,
446 which include three variant sets containing putatively causal regulatory variants derived from statistical as-
447 sociations (i.e. Allelic imbalanced SNPs, Fine mapping eQTLs, GWAS significant noncoding SNPs), and
448 three datasets consisting of experimentally validated regulatory variants (i.e. Experimentally validated reg-
449 ulatory SNPs, MPRA validated variants in GM12878 lymphoblastoid cells, MPRA validated variants in
450 K562 leukemia cells). Besides evaluating context-dependent WEVar in each benchmark dataset by divid-
451 ing it into training and testing set, we adapt an independent training and testing set from CAGI. Conse-
452 quently, both context-free and context-dependent WEVar achieve an overall improvement of functional

453 prediction compared to integrated scoring methods across all datasets. Specifically, WEVar outperforms
454 Unweighted average, indicating the benefit of exploiting the optimized contributions of individual scoring
455 method. GWAVA_Unmatched and Unweighted average are top-performed. In contrast, DANN, CADD
456 and FATHMM_MKL always perform poorly. By comparing context-free and context-dependent WEVar
457 on the same benchmark datasets, we find that context-dependent WEVar improve the functional predic-
458 tion compared to context-free WEVar except for Experimentally validated regulatory SNPs possibly to the
459 small sample size of training set. This observation indicates that being context-dependent improves the
460 functional prediction and a large sample size is needed for make this improvement.

461 Another important characteristic of WEVar is that it can identify predictors that play major contribution
462 to the functional prediction. As a result, major contributors are different across benchmark datasets. In
463 most cases, WEVar identifies a parsimonious set of scoring methods that dominate the functional prediction
464 especially FunSeq2 and GWAVA_Unmatched are two ubiquitous major contributors. However, for GWAS
465 noncoding SNPs and MPRA validated regulatory variants in K562 leukemia cells, there is a ubiquitous
466 solution, where the contributions of all methods are relative uniform. These findings demonstrate that both
467 estimated weights and major contributors vary from context to context. Thus, it is important to obtain
468 an optimal weights when integrating different scoring methods, as the non-uniform weights estimated by
469 WEVar lead improved functional prediction across benchmark datasets. Additionally, this point is validated
470 by both simulation and real data applications that WEVar outperforms the unweighted average of functional
471 scores.

472 To demonstrate the application of WEVar in complex traits, we apply WEVar in the fine mapping analy-
473 sis to evaluate whether it can successfully prioritize causal regulatory variants among LD-linked noncoding
474 variants. By using precomputed WEVar score directly, variants assigned the highest score in a risk locus is
475 considered to be prioritized. By using three benchmarking datasets of experimentally validated regulatory
476 variants, we find that WEVar can prioritize regulatory variants modulating gene expression in GM12878
477 lymphoblastoid cells, associated with Schizophrenia and multiple traits such as Cleft lip/palate, heart, hair
478 color and breast cancer. These findings demonstrate that WEVar can prioritize functional noncoding vari-
479 ants in risk loci and therefore alleviate the limitation of current GWAS, where the true causal SNPs may be
480 masked by LD.

481 WEVar is a flexible approach, which can be further extended and improved by both integrated scoring

482 methods and training variant set. In the current implementation, we include several representative scor-
483 ing methods that are most popular in this field. With the rapid development post-GWAS analysis, there
484 are other powerful methods developed or developing can be integrated into WEVar to further improve the
485 prediction performance. The flexibility of WEVar is also reflected on the training variant set. With the
486 affordability and popularity of functional assays such as massively parallel reporter assays (MPRAs) and
487 clustered regularly interspaced short palindromic repeats (CRISPR)-based gene editing, more experimen-
488 tally validated functional variants can be discovered and integrated into WEVar to improve the predictive
489 power.

490 Methods

491 WEVar is developed directly on top of precomputed functional score, which is an optimally integrative met-
492 ric representing for thousands of functional annotations, from multiple individual scoring methods. Using
493 these integrative functional scores directly will decrease the number of features in the model development
494 and thus avoid the challenge high-dimensional data and multicollinearity. We will outline the details of
495 WEVar in the following sessions.

496 Obtaining precomputed functional scores

497 We download base-level genome-wide precomputed functional scores from all possible substitutions of
498 single nucleotide variants (SNVs) in the human reference genome (GRCh37/hg19) from scoring methods
499 including CADD [16], DANN [17], FunSeq2 [20], FATHMM-MKL [18], Eigen [21] and LINSIGHT [19].
500 In addition, we use three sets of precomputed scores from GWAVA (i.e. GWAVA_region, GWAVA_TSS,
501 GWAVA_unmatched) for all SNVs in 1000 Genomes Project [22]. We choose these scoring methods to
502 integrate into WEVar because they are widely used and mostly representative. Since the precomputed score
503 of LINSIGHT is on region level, we assign all variants in the region with the same region-level score. More
504 details for the source of these precomputed scores can be found in Table S13.

505 Assembling variants in training and testing set

506 For context-free WEVar, the training variant set compiles a curated set of 5,247 causal regulatory vari-
507 ants including i) deleterious or pathogenic noncoding variants from the Human Gene Mutation Database

508 (HGMD) [25] and ClinVar [44] ii) validated regulatory noncoding variants from the OregAnno [45] and
509 iii) candidate causal SNPs for 39 immune and non-immune diseases in the fine-mapping study [46] ob-
510 tained from Li et al. [26]. The compiled variants are associated with different traits, have functional con-
511 sequence in different tissues and cell types, and reside in different noncoding regions such as promoters,
512 enhancers, 5'UTRs and 3'UTRs, making them ideal as a training set to predict functional consequence of
513 noncoding variants from unknown or heterogeneous context. Accordingly, we collect six state-of-the-art
514 benchmark independent variant sets from a wide range of context. Among them, three variant sets are
515 collected from Li et al. [26], which include experimentally validated regulatory variants, expression quanti-
516 tative trait loci (eQTL) [29] ($FDR < 0.1\%$) and allelic imbalanced SNPs [28] ($FDR < 0.1\%$) Moreover, GWAS
517 significant noncoding SNPs are collected from NHGRI-EBI GWAS Catalog [30] ($pvalue < 10^{-5}$). Further-
518 more, two collected regulatory variant sets are validated by massively parallel reporter assays (MPRAs) in
519 GM12878 lymphoblastoid cells [32] and K562 leukemia cells [33]. For context-free WEVar, these variant
520 sets are used for independent testing. For context-dependent WEVar, we divide each variant set into ten
521 folds with nine-folds as training set and one-fold as testing set.

522 **Statistical learning framework of WEVar**

523 The workflow of WEVar is illustrated in Figure 1, which consists of four steps: (i) Creating the compiled
524 training variant set (ii) Obtaining the precomputed functional scores for training variants (iii) Transforming
525 the functional scores (iv) Training a constraint ensemble model.

526 **Creating compiled training variant set**

527 Depending on the purpose, we compile the training set for either "context-free" or "context-dependent"
528 WEVar, as described in the section "Assembling variants in training and testing set".

529 **Obtaining precomputed functional scores for training variants**

530 Precomputed functional scores are retrieved from representative scoring methods including CADD, DANN,
531 Eigen, FunSeq2, FATHMM-MKL, LINSIGHT and GWAFA for variants in the training set, as described in
532 the section "Obtaining precomputed functional scores".

533 **Transforming precomputed functional scores**

534 Precomputed functional scores of integrated scoring methods are on different scales, which may result in
535 different effect sizes of weight estimates by WEVar. However, the resulted different weight estimates are not
536 due to different contributions of integrated scoring methods but because of the systematic bias induced by
537 score scale. Therefore, it is important to perform a normalization step to make functional scores from differ-
538 ent scales comparable. To integrate different scores are on the same scale, for each j th scoring method, we
539 estimate two probability density functions (PDF) using kernel density estimation (KDE) based on the em-
540 pirical distribution of the normalized scores for positive variant set and negative set respectively. As a result,
541 PDF of the positive set denoted as $\mathbf{p}_j(s|+)$ approximates the probability that a variant will have a prediction
542 score s given the variant is functional (+), while PDF of the negative set denoted as $\mathbf{p}_j(s|-)$ approximates
543 the probability that a variant will have the same prediction score s given the variant is nonfunctional (-).
544 Therefore, we use the ratio of two PDFs for the given i th variant, which is essentially the Bayes factor, to rep-
545 resent the likelihood the variant is functional versus nonfunctional. To stabilize the scale of the likelihood,
546 we further take a logarithm of the ratio as the transformed score x_{ij}^N as:

547

$$x_{ij}^N = \log \frac{\mathbf{p}_j(x_{ij}|+)}{\mathbf{p}_j(x_{ij}|-)} \quad (5)$$

548 where x_{ij} is the raw functional score of the i th variant in the j th scoring method; $\mathbf{p}_j(x_{ij}|+)$ and $\mathbf{p}_j(x_{ij}|-)$
549 are probability density of x_{ij} in positive and negative set respectively.

550 **Training a constraint ensemble model**

551 Using the transformed scores, we will fit a constraint ensemble model, which is essentially a Constrained
552 Penalized Logistic Regression model. Let $\mathbf{x}^N \in \mathbb{R}^p$ be the transformed scores of a variant for all scoring
553 methods and $y \in \{-1, +1\}$ be the variant label. The conditional probability of the variant being functional
554 given \mathbf{x}^N can be formulated as:

555

$$\mathbf{p}(y = 1|\mathbf{x}^N) = \frac{1}{1 + \exp(-y(\mathbf{w}^\top \mathbf{x}^N) + b)} \quad (6)$$

556 where $\mathbf{w} \in \mathbb{R}^p$ is a weight vector, which contains the regression coefficients, and $b \in \mathbb{R}$ is the intercept.
557 The likelihood function for n variants from both positive and negative set is defined as $\prod_{i=1}^n \mathbf{p}(y_i|\mathbf{x}_i^N)$. The

558 objective function, which is the average of negative log-likelihood, is defined as:

$$559 \quad f(\mathbf{w}, \mathbf{b}) = -\frac{1}{n} \log \prod_{i=1}^n \mathbf{p}(y_i | \mathbf{x}_i^N) \quad (7)$$

560 By minimizing the objective function, we can estimate \mathbf{w} and b as:

$$561 \quad \underset{\mathbf{w}, b}{\text{minimize}} \quad f(\mathbf{w}, b) \quad (8)$$

562 We further apply two constraints to the log-likelihood function. First, the weight of each scoring method
 563 is larger or equal to 0, indicating all scoring methods will contribute neutrally or positively to the prediction.
 564 Second, the sum of all weights equals to 1, which is a reasonable assumption for the summation of
 565 contributions from all scoring methods. In addition, to leverage all scoring methods by avoiding a sparse
 566 solution, we add an L_2 -norm to the objective function. Finally, we have the L_2 -norm regularized objective
 567 function with the two constraints as:

$$568 \quad \begin{aligned} & \underset{\mathbf{w}, b}{\text{minimize}} \quad f(\mathbf{w}, b) + \lambda \|\mathbf{w}\|_2 \\ & \text{subject to} \quad \sum_{j=1}^p \mathbf{w}_j = 1 \\ & \quad \mathbf{w}_j \geq 0, \quad j = 1, \dots, p. \end{aligned} \quad (9)$$

569 where $\lambda \geq 0$ is the tuning parameter for L_2 -norm, which can be optimized from cross-validation in the
 570 training phase.

571 To minimize the loss function with equality and inequality constraints, we first rewrite the loss function
 572 as the standard form:

$$573 \quad \begin{aligned} & \underset{\mathbf{w}, b}{\text{minimize}} \quad f(\mathbf{w}, b) + \lambda \|\mathbf{w}\|_2 \\ & \text{subject to} \quad h_k(\mathbf{w}) \leq 0, \quad k = 1, \dots, p. \\ & \quad l(\mathbf{w}) = 0 \end{aligned} \quad (10)$$

574 We then introduce Generalized Lagrange function to relax two constraints, which is formulated as:

$$575 \quad \mathcal{L}(\mathbf{w}, b, \alpha, \beta) = f(\mathbf{w}, b) + \lambda \|\mathbf{w}\|_2 + \sum_{k=1}^p \alpha_k h_k(\mathbf{w}) + \beta l(\mathbf{w}) \quad (11)$$

⁵⁷⁶ In this way, the dual problem is easier to solve compared with the primal problem. The primal solution can
⁵⁷⁷ be constructed from the dual solution as:

$$g(\alpha, \beta) = \min \mathcal{L}(\mathbf{w}, b, \alpha, \beta) \quad (12)$$

⁵⁷⁹ The Lagrange dual function can be considered as a pointwise maximization of some affine functions so it is
⁵⁸⁰ always concave. The dual problem is always convex even if the primal problem is not convex, which can be
⁵⁸¹ easily solved by gradient-based methods.

⁵⁸² Testing phase

⁵⁸³ In the testing phase, given variants be annotated precomputed functional scores from all scoring methods,
⁵⁸⁴ which will be further transformed through the estimated KDE in the training phase. The transformed scores
⁵⁸⁵ will serve as input features for trained ensemble model to predict the ensemble WEVar score.

⁵⁸⁶ Implementation

⁵⁸⁷ We adopt the SciPy [47], a Python scientific computing library, to perform the kernel density estimations,
⁵⁸⁸ and CVXPY [48], a Python-embedded modeling library for convex optimization, to estimate constrained
⁵⁸⁹ weights from the objective function.

⁵⁹⁰ Software availability

⁵⁹¹ WEVar is implemented in a standalone software toolkit available at (<https://github.com/lichen-lab/WEVar>), which mainly consists of i) a compiled data package including precomputed scores for all SNVs
⁵⁹² (GRCh37/hg19) in 1000 Genomes Project across all integrated scoring methods; ii) a model package of pre-
⁵⁹³ trained context-free and context-dependent WEVar models; and iii) a Python software package to perform
⁵⁹⁴ the functional prediction using pre-trained models or re-train a new model. To use a pre-trained model,
⁵⁹⁵ WEVar will take compiled data package and genomic coordinates of testing variants as input. Alternatively,
⁵⁹⁶ WEVar will take compiled data package and genomic coordinates of training variants to re-train a new
⁵⁹⁷ WEVar model.
⁵⁹⁸

599 Acknowledgments

600 This work was supported by the Indiana University Precision Health Initiative and Showalter Research Trust
601 Fund [to L.C.] and the National Institute of Health R35 GM138342 [to Y.J.].

602 Conflict of interest statement

603 None declared.

604 References

- 605 [1] JK Pickrell, JC Marioni, AA Pai, JF Degner, BE Engelhardt, E Nkadori, JB Veyrieras, M Stephens, Y
606 Gilad, and JK Pritchard. Understanding mechanisms underlying human gene expression variation
607 with RNA sequencing. *Nature*. **464**: 768–72.
- 608 [2] JR Gibbs, MP van der Brug, DG Hernandez, BJ Traynor, MA Nalls, SL Lai, S Arepalli, A Dillman,
609 IP Rafferty, J Troncoso, et al. Abundant quantitative trait loci exist for DNA methylation and gene
610 expression in human brain. *PLoS Genet*. **6**: e1000952.
- 611 [3] EB Josephs, YW Lee, JR Stinchcombe, and SI Wright. Association mapping reveals the role of puri-
612 fying selection in the maintenance of genomic variation in gene expression. *Proc Natl Acad Sci U S
613 A*. **112**: 15390–5.
- 614 [4] JF Degner, AA Pai, R Pique-Regi, JB Veyrieras, DJ Gaffney, JK Pickrell, S De Leon, K Michelini, N
615 Lewellen, GE Crawford, et al. DNase I sensitivity QTLs are a major determinant of human expression
616 variation. *Nature*. **482**: 390–4.
- 617 [5] A Takata, N Matsumoto, and T Kato. Genome-wide identification of splicing QTLs in the human
618 brain and their enrichment among schizophrenia-associated loci. *Nat Commun*. **8**: 14519.
- 619 [6] PJ Killela, ZJ Reitman, Y Jiao, C Bettegowda, N Agrawal, J Diaz L. A., AH Friedman, H Friedman,
620 GL Gallia, BC Giovanella, et al. TERT promoter mutations occur frequently in gliomas and a subset
621 of tumors derived from cells with low rates of self-renewal. *Proc Natl Acad Sci U S A*. **110**: 6021–6.

622 [7] MR Mansour, BJ Abraham, L Anders, A Berezovskaya, A Gutierrez, AD Durbin, J Etchin, L Lawton,
623 SE Sallan, LB Silverman, et al. Oncogene regulation. An oncogenic super-enhancer formed through
624 somatic mutation of a noncoding intergenic element. *Science*. **346**: 1373–7.

625 [8] L Chen, P Jin, and ZS Qin. DIVAN: accurate identification of non-coding disease-specific risk vari-
626 ants using multi-omics profiles. *Genome Biol.* **17**: 252.

627 [9] EP Consortium. An integrated encyclopedia of DNA elements in the human genome. *Nature*. **489**:
628 57–74.

629 [10] C Roadmap Epigenomics, A Kundaje, W Meuleman, J Ernst, M Bilenky, A Yen, A Heravi-Moussavi, P
630 Kheradpour, Z Zhang, J Wang, et al. Integrative analysis of 111 reference human epigenomes. *Nature*.
631 **518**: 317–30.

632 [11] HG Stuinenberg, C International Human Epigenome, and M Hirst. The International Human Epigenome
633 Consortium: A Blueprint for Scientific Collaboration and Discovery. *Cell*. **167**: 1897.

634 [12] L Chen and ZS Qin. Using DIVAN to assess disease/trait-associated single nucleotide variants in
635 genome-wide scale. *BMC Res Notes*. **10**: 530.

636 [13] L Chen, Y Wang, B Yao, A Mitra, X Wang, and X Qin. TIVAN: tissue-specific cis-eQTL single nu-
637 cleotide variant annotation and prediction. *Bioinformatics*. **35**: 1573–1575.

638 [14] L Chen and ZS Qin. traseR: an R package for performing trait-associated SNP enrichment analysis
639 in genomic intervals. *Bioinformatics*. **32**: 1214–6.

640 [15] GR Ritchie, I Dunham, E Zeggini, and P Flück. Functional annotation of noncoding sequence vari-
641 ants. *Nature methods*. **11**: 294.

642 [16] P Rentzsch, D Witten, GM Cooper, J Shendure, and M Kircher. CADD: predicting the deleteriousness
643 of variants throughout the human genome. *Nucleic acids research*. **47**: D886–D894.

644 [17] D Quang, Y Chen, and X Xie. DANN: a deep learning approach for annotating the pathogenicity of
645 genetic variants. *Bioinformatics*. **31**: 761–763.

646 [18] HA Shihab, MF Rogers, J Gough, M Mort, DN Cooper, IN Day, TR Gaunt, and C Campbell. An in-
647 tegrative approach to predicting the functional effects of non-coding and coding sequence variation.
648 *Bioinformatics*. **31**: 1536–1543.

649 [19] YF Huang, B Gulko, and A Siepel. Fast, scalable prediction of deleterious noncoding variants from
650 functional and population genomic data. *Nature genetics*. **49**: 618.

651 [20] Y Fu, Z Liu, S Lou, J Bedford, XJ Mu, KY Yip, E Khurana, and M Gerstein. FunSeq2: a framework
652 for prioritizing noncoding regulatory variants in cancer. *Genome biology*. **15**: 480.

653 [21] I Ionita-Laza, K McCallum, B Xu, and JD Buxbaum. A spectral approach integrating functional ge-
654 nomic annotations for coding and noncoding variants. *Nature genetics*. **48**: 214.

655 [22] 1GP Consortium et al. An integrated map of genetic variation from 1,092 human genomes. *Nature*.
656 **491**: 56.

657 [23] L Koch. Exploring human genomic diversity with gnomAD. *Nat Rev Genet*. **21**: 448.

658 [24] L Liu, MD Sanderford, R Patel, P Chandrashekhar, G Gibson, and S Kumar. Biological relevance of
659 computationally predicted pathogenicity of noncoding variants. *Nat Commun*. **10**: 330.

660 [25] PD Stenson, M Mort, EV Ball, K Shaw, AD Phillips, and DN Cooper. The Human Gene Mutation
661 Database: building a comprehensive mutation repository for clinical and molecular genetics, diag-
662 nostic testing and personalized genomic medicine. *Human genetics*. **133**: 1–9.

663 [26] MJ Li, Z Pan, Z Liu, J Wu, P Wang, Y Zhu, F Xu, Z Xia, PC Sham, JPA Kocher, et al. Predicting
664 regulatory variants with composite statistic. *Bioinformatics*. **32**: 2729–2736.

665 [27] J Wang, AZ Dayem Ullah, and C Chelala. IW-Scoring: an Integrative Weighted Scoring framework
666 for annotating and prioritizing genetic variations in the noncoding genome. *Nucleic Acids Res*. **46**:
667 e47.

668 [28] MT Maurano, E Haugen, R Sandstrom, J Vierstra, A Shafer, R Kaul, and JA Stamatoyannopoulos.
669 Large-scale identification of sequence variants influencing human transcription factor occupancy in
670 vivo. *Nature genetics*. **47**: 1393.

671 [29] CD Brown, LM Mangravite, and BE Engelhardt. Integrative modeling of eQTLs and cis-regulatory
672 elements suggests mechanisms underlying cell type specificity of eQTLs. *PLoS genetics*. **9**:

673 [30] A Buniello, JAL MacArthur, M Cerezo, LW Harris, J Hayhurst, C Malangone, A McMahon, J Morales,
674 E Mountjoy, E Sollis, et al. The NHGRI-EBI GWAS Catalog of published genome-wide association
675 studies, targeted arrays and summary statistics 2019. *Nucleic Acids Res*. **47**: D1005–D1012.

676 [31] Z He, L Liu, K Wang, and I Ionita-Laza. A semi-supervised approach for predicting cell-type specific
677 functional consequences of non-coding variation using MPRAs. *Nature communications*. **9**: 1–12.

678 [32] R Tewhey, D Kotliar, DS Park, B Liu, S Winnicki, SK Reilly, KG Andersen, TS Mikkelsen, ES Lan-
679 der, SF Schaffner, et al. Direct identification of hundreds of expression-modulating variants using a
680 multiplexed reporter assay. *Cell*. **165**: 1519–1529.

681 [33] P Kheradpour, J Ernst, A Melnikov, P Rogov, L Wang, X Zhang, J Alston, TS Mikkelsen, and M Kellis.
682 Systematic dissection of regulatory motifs in 2000 predicted human enhancers using a massively
683 parallel reporter assay. *Genome research*. **23**: 800–811.

684 [34] A Kreimer, H Zeng, MD Edwards, Y Guo, K Tian, S Shin, R Welch, M Wainberg, R Mohan, NA
685 Sinnott-Armstrong, et al. Predicting gene expression in massively parallel reporter assays: A com-
686 parative study. *Hum Mutat*. **38**: 1240–1250.

687 [35] MJ Machiela and SJ Chanock. LDlink: a web-based application for exploring population-specific
688 haplotype structure and linking correlated alleles of possible functional variants. *Bioinformatics*. **31**:
689 3555–7.

690 [36] B Moreno-Kustner, C Martin, and L Pastor. Prevalence of psychotic disorders and its association with
691 methodological issues. A systematic review and meta-analyses. *PLoS One*. **13**: e0195687.

692 [37] S Saha, D Chant, J Welham, and J McGrath. A systematic review of the prevalence of schizophrenia.
693 *PLoS Med*. **2**: e141.

694 [38] GBD Disease, I Injury, and C Prevalence. Global, regional, and national incidence, prevalence, and
695 years lived with disability for 328 diseases and injuries for 195 countries, 1990–2016: a systematic
696 analysis for the Global Burden of Disease Study 2016. *Lancet*. **390**: 1211–1259.

697 [39] L Myint, R Wang, L Boukas, KD Hansen, LA Goff, and D Avramopoulos. A screen of 1,049 schizophre-
698 nia and 30 Alzheimer’s-associated variants for regulatory potential. *Am J Med Genet B Neuropsychiatr
699 Genet*. **183**: 61–73.

700 [40] M van den Boogaard et al. A common genetic variant within SCN10A modulates cardiac SCN5A
701 expression. *J Clin Invest*. **124**: 1844–52.

702 [41] EJ Leslie, MA Taub, H Liu, KM Steinberg, DC Koboldt, Q Zhang, JC Carlson, JB Hetmanski, H Wang,
703 DE Larson, et al. Identification of functional variants for cleft lip with or without cleft palate in or
704 near PAX7, FGFR2, and NOG by targeted sequencing of GWAS loci. *Am J Hum Genet.* **96**: 397–411.

705 [42] CA Guenther, B Tasic, L Luo, MA Bedell, and DM Kingsley. A molecular basis for classic blond hair
706 color in Europeans. *Nat Genet.* **46**: 748–52.

707 [43] S Liu, Y Liu, Q Zhang, J Wu, J Liang, S Yu, GH Wei, KP White, and X Wang. Systematic identification
708 of regulatory variants associated with cancer risk. *Genome Biol.* **18**: 194.

709 [44] MJ Landrum, JM Lee, GR Riley, W Jang, WS Rubinstein, DM Church, and DR Maglott. ClinVar: pub-
710 lic archive of relationships among sequence variation and human phenotype. *Nucleic acids research.*
711 **42**: D980–D985.

712 [45] OL Griffith, SB Montgomery, B Bernier, B Chu, K Kasaian, S Aerts, S Mahony, MC Sleumer, M
713 Bilenky, M Haeussler, et al. ORegAnno: an open-access community-driven resource for regulatory
714 annotation. *Nucleic acids research.* **36**: D107–D113.

715 [46] KKH Farh, A Marson, J Zhu, M Kleinewietfeld, WJ Housley, S Beik, N Shores, H Whitton, RJ Ryan,
716 AA Shishkin, et al. Genetic and epigenetic fine mapping of causal autoimmune disease variants. *Na-
717 ture.* **518**: 337.

718 [47] E Jones, T Oliphant, P Peterson, et al. SciPy: Open source scientific tools for Python. 2001.

719 [48] S Diamond and S Boyd. CVXPY: A Python-Embedded Modeling Language for Convex Optimiza-
720 tion. *Journal of Machine Learning Research.* **17**: 1–5.